New Beyond-Mean-Field Theories: Examination of the Potential Shell Closures at $N = 32$ or 34

Tomás R. Rodríguez and J. Luis Egido
Departamento de Física Teórica, Universidad Autónoma de Madrid, E-28049 Madrid, Spain
(Received 14 March 2007; published 6 August 2007)

A beyond-mean-field theory of new generation has been developed and applied for the first time to discuss the controversial $N = 32$ and/or $N = 34$ shell closures and the puzzling behavior of the transition probabilities from the ground to the first 2^+ state in the titanium isotopes. In the numerical applications, the finite range density dependent Gogny interaction has been used. As compared with the experimental data for several calcium, titanium, and chromium isotopes, we obtain a good agreement for the excitation energies and a reasonable one for the transition probabilities. Our calculations support a shell closure for $N = 32$ but not for $N = 34$.

DOI: 10.1103/PhysRevLett.99.062501 PACS numbers: 21.60.Jz, 21.10.Re, 21.60.Ev, 27.40.+z

New developments in radioactive nuclear beams and gamma ray detectors have allowed the study of atomic nuclei far from the beta line of stability. From the theoretical point of view, the study of such exotic systems has favored the development of more elaborated many body theories. Among other interesting properties, the appearance of new magic numbers [1] or the degradation of the conventional ones in exotic nuclei is one of the major research fields of the nuclear structure community. Recently, a new shell closure at $N = 32$ in the neutron rich Ca, Ti, and Cr isotope chains has been studied both theoretically and experimentally. The experimental systematics of the energies of the first 2_1^+ states in the Ca [2], Ti [3–6], and Cr [7,8] isotopic chains, and also of the $B(E2, 0_1^+ \rightarrow 2_1^+)$ in Ti [9] and Cr [10], are consistent with a shell closure at $N = 32$. Large scale shell model calculations have been performed in the pf shell with two different families of effective interactions, namely, GXPF1 [11] and KB3G [12]. All the calculations are in agreement with the experimental trend of the energies of the 2_1^+ states up to $N = 32$ although the GXPF1 interaction predicts another shell closure at $N = 34$ which is not observed in ^{56}Ti and ^{58}Cr [3,7,13]. The crucial nucleus ^{54}Ca has not been measured yet. Concerning the transitional probabilities, none of both interactions is able to reproduce the zigzag behavior of the $B(E2; 0_1^+ \rightarrow 2_1^+)$ values observed in the Titanium isotopes with the usual effective charges.

An alternative approach to the large scale shell model calculations are the mean field based many body theories [14]. These theories have been traditionally applied to heavy nuclei, and the treatment of light, exotic nuclei requires special consideration. A characteristic of these nuclei is that as one leaves the stability line, the potential energy surface softens in most degrees of freedom, and the mean field approximation, even in its most sophisticated version like the Hartree-Fock-Bogoliubov (HFB), is not a good approximation anymore and additional residual interactions must be considered. This is usually done in the so-called Beyond-Mean-Field Approximations (BMFA). This approach incorporates residual interactions of different type. On the one hand, those associated with the restoration of the symmetries spontaneously broken in the HFB approach, like angular momentum and particle number. On the other hand, configuration mixing to include fluctuations of small and large amplitude of the main degrees of freedom. Up to now, due to limitations of the numerical feasibility, only the quadrupole deformations are considered explicitly. In the plain HFB approach, one explores the quadrupole potential energy surface for a large set of discrete values of q ($q_i = 1, \ldots, M$) by minimizing $E'' = \langle\varphi|\hat{H}' - \lambda_q\hat{Q}|\varphi\rangle/\langle\varphi|\varphi\rangle$, with λ_q the Lagrange multiplier determined by the constraint $\langle\varphi|\hat{Q}|\varphi\rangle/\langle\varphi|\varphi\rangle = q$ and $\hat{H}' = \hat{H} - \lambda_N\hat{N} - \lambda_Z\hat{Z}$ in an obvious notation. The wave function (WF) φ is of the HFB type. To recover the particle and rotational invariance broken in the HFB approach, a projection on the corresponding quantum numbers takes place to obtain the WF $|\Phi(q)\rangle = \hat{P}^J\hat{P}^N|\varphi(q)\rangle$ with $\hat{P}^J$ ($\hat{P}^N$) an operator which projects $|\varphi(q)\rangle$ onto an eigenstate of the angular momentum (particle number) operator. At the end, these calculations amount to determine a set of highly correlated WF's $\{|\Phi(q_i)\rangle\}$ -depending parametrically on the variables q_i- as a basis to diagonalize the nuclear Hamiltonian. This pattern, with small variations, is the one followed by all BMFA calculations performed so far [14–16]. These kinds of approaches have a drawback in the treatment of the pairing correlations. The HFB approach with or without particle number projection works properly in the regime of strong pairing correlations, but it breaks down in the weak pairing regime. The Lipkin-Nogami (LN) [17] approximation partially cures this deficiency but not completely. The real solution to this problem is well known [18,19]; namely, one has to minimize the particle number projected energy in order to minimize the energy of the nucleus we are interested in—this is the so-called Variation After Projection (VAP) method—instead of minimizing the energy of an admixture of nuclei with different number of particles, as it does in the HFB approach.

The purpose of this Letter is twofold: first, to incorporate the particle number projection in configuration mixing

calculations with the Gogny force, which so far [15] has not been done, and second and more important, to introduce for the first time the above mentioned VAP effects in BMFA theories. As a test, we shall apply the new theory to the challenging problem of the $N = 32$ and $N = 34$ shell closures and the intriguing problem of the effective charges in the Titanium isotopes [20]. Specifically, in our approach, we proceed in the following way: for each q value, we minimize the particle number projected (PNP) HFB energy $E'^N(q) = \langle\varphi(q)|(\hat{H} - \lambda_q \hat{Q})P^N|\varphi(q)\rangle / \langle\varphi(q)|P^N|\varphi(q)\rangle$ with the corresponding constraint on the expectation value of $\hat{Q}$. Later on, we diagonalize $\hat{H}$ in the subspace spanned by the WF's $P^N P^J|\varphi(q)\rangle$ for a wide range of q-values. We restrict ourselves to axial symmetry in all steps of the calculations. We use a large configuration space of eleven harmonic oscillator shells (we do not need therefore effective charges) and the standard parametrization D1S of the Gogny force [21]. We also take into account *all* exchange terms of the force to avoid the well-known problem associated with the divergences appearing in a particle number projected theory [22]. The presence of divergences is specially critical for all BMFAs since the parameter q must be changed in a continuous way.

Pairing correlations depend very much on the single particle level density around the Fermi level. In the upper panels of Fig. 1, we display as an example the single particle energies in the HFB approach for the nucleus ^{54}Cr. If we follow the Fermi level for protons or neutrons, we find on the oblate side relatively high level density and a very low one in several regions on the prolate side. It is well known that the HFB approach provides a good approximation in the strong pairing regime and a very poor one in the weak pairing regime. As a consequence, we expect an oscillating degree of quality of the HFB approach as a function of q; in particular, one finds a spurious superfluid normal-fluid phase transition for those q-values for which the level density is extremely small. This can be seen in the bottom panels of Fig. 1 where the HFB pairing correlations have been plotted. As expected from the upper panels, the proton pairing correlations vanish for $1.2\ \text{b} \leq q \leq 2.4\ \text{b}$ and for the neutron around $q \approx 1.1$ b. This situation presents a serious drawback and needs to be improved. The projected Lipkin-Nogami which is used as a remedy by some authors [14,16] might not help much in these situations since this method is known to provide a bad approach in the weak pairing regime [17]. A thorough comparison between different approaches to the treatment of pairing correlations will be published elsewhere [23]. In the bottom panels, the pairing energies in the PNP-HFB approach are also shown. The neutron and proton systems illustrate clearly how this approach works. In the regions where the HFB pairing correlations are sizable, the PNP-HFB approach provides additional correlations of about 2 MeV, and in the regions where they vanish or are very small, the additional correlations amount to 4 to 5 MeV. As

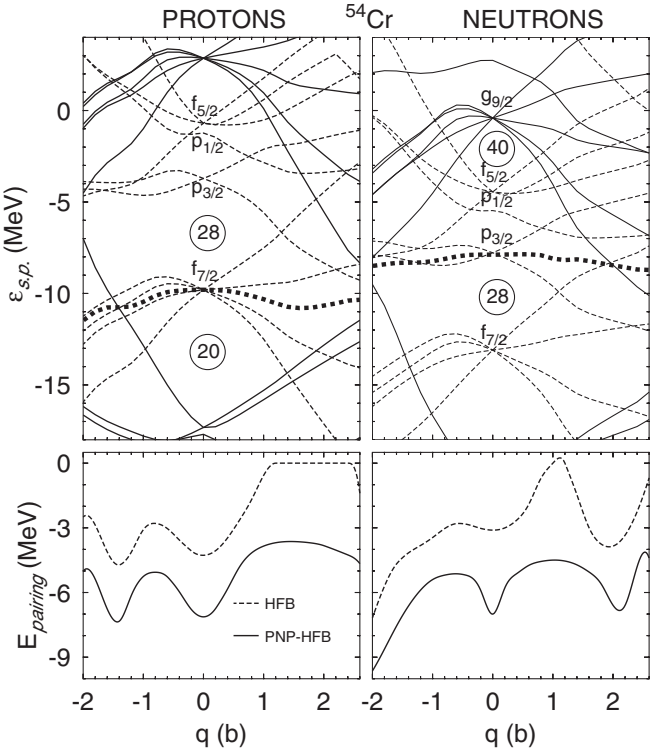

FIG. 1. Upper panels: Single particle energies of protons (left) and neutrons (right) for the nucleus ^{54}Cr as a function of the quadrupole moment. Positive (negative) parity levels are represented by continuous (dashed) lines. Thick dotted lines represent the Fermi levels. Lower panels: Pairing energies for protons (left) and neutrons (right) in two approaches.

we will see in Fig. 2, the q values where the differences between the HFB and the PNP-HFB are larger are very relevant since they correspond to the energy minima.

One can get some insight in the physics of the shell closures problem posed above by looking at the intrinsic potential energy curves, which are plotted in Fig. 2 in the PNP-HFB approach for the Ca, Ti, and Cr isotopes for neutron number 28, 30, 32, and 34. The Calcium isotopes display the steepest curves due to the $Z = 20$ proton shell closure, and for increasing proton number, we find a broadening of the curves, i.e., an increase of collectivity. Concerning the shell closures, the dependence on the neutron number is more interesting. For all three elements, we find the curves for $N = 28, 32$ to behave differently from the ones for $N = 30, 34$. The next interesting question concerns the role played by the residual interactions brought in by the angular momentum projection and the configuration mixing effects.

As an example, we display in Fig. 3 the angular momentum projected energy curves for the nucleus ^{54}Cr. Specifically, we are plotting the quantity $E^{J,N}(q) = \langle\varphi(q)|\hat{H}P^J P^N|\varphi(q)\rangle / \langle\varphi(q)|P^J P^N \varphi(q)\rangle$ for different q values. As a reference, the PNP-HFB curve is also represented. In the left panel, the results for $J = 0^+\hbar$ are shown; the angular momentum projection gives an additional energy lowering with respect to the PNP-HFB result,

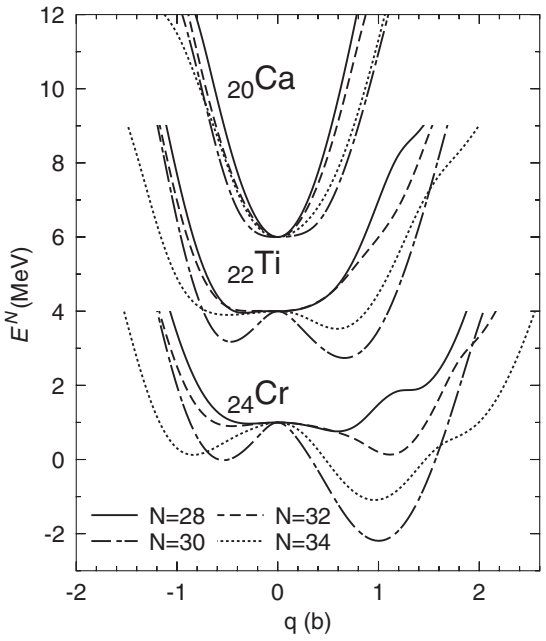

FIG. 2. Potential energy surfaces in the PNP-HFB approach as a function of the quadrupole moment. The energy origin of the isotopes of each element has been set at the same value, Cr at 1 MeV, Ti at 4 MeV, and Ca at 6 MeV. At large q-values, the energies are not displayed to keep the plot readable.

of a few MeV. The prolate and oblate minima are slightly shifted to larger q values, and the energy gain amounts to 3 MeV in both minima. The energy lowering for $J = 2^+\hbar$ (see right panel) is in general smaller than for $J = 0^+\hbar$. The shift to larger q values also takes place, but the energy gain for the prolate minimum is 1 MeV larger than for the oblate one. The projected curves are, so to say, the diagonal elements of the matrix to be diagonalized in the configuration mixing calculations. The diagonalization of these matrices for different J values provides the eigenvalues and the eigenstates we are looking for. In Fig. 3, we have plotted the energies and the wave functions for the 0_1^+ and 2_1^+ states. The configuration mixing provides an additional energy lowering with respect to the minimum of the projected surface of 0.60 MeV for the 0_1^+ state and 0.32 MeV for the 2_1^+. The wave functions indicate that the 0_1^+ state is a superposition of prolate shapes peaked at 1.2 b and a small admixture of oblate ones. The wave function of the 2_1^+ state looks similar to the one of the 0_1^+ state though it has less oblate mixing. With these wave functions, one calculates properties like transition probabilities, spectroscopic moments, and so on. It is important to notice that the q-value where the collective WF peaks is the one where the HFB approach provides the worst approximation, cf. Figure 1.

We have performed the same analysis for all nuclei we are interested in, and the results for the energies of the 2_1^+ states are plotted in Fig. 4 for some isotopes of the nuclei Cr, Ti, and Ca together with the experimental data. The theoretical predictions display the same behavior as the

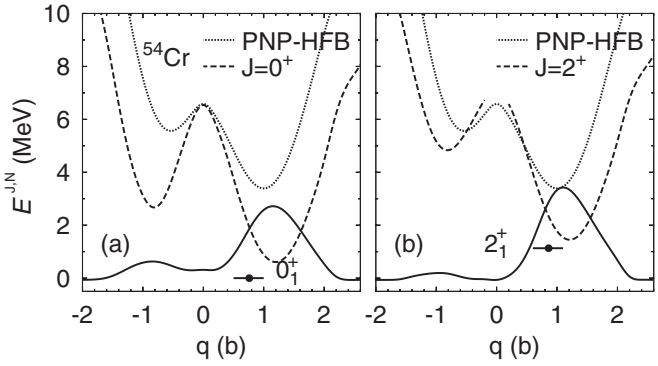

FIG. 3. Angular momentum projected energy surfaces (dashed lines) and energies (bullets) and collective wave functions in arbitrary units (continuous lines) of the configuration mixing calculation for $J = 0_1^+\hbar$ (left) and $J = 2_1^+\hbar$ (right) states. The abscissa of the bullets represents the intrinsic deformation parameter. To fix an absolute scale for both panels, the energy of the 0_1^+ state has been set equal to zero.

experimental data though they are a bit larger. As discussed on p. 290 of [24], this is caused in part by the lack of triaxiality effects in our calculations. The largest effect is expected for spherical nuclei and the smallest one for well deformed ones ,and this is also the case here, cf. Fig. 2. In Ref. [24], we estimated that a factor of about 0.7 is needed

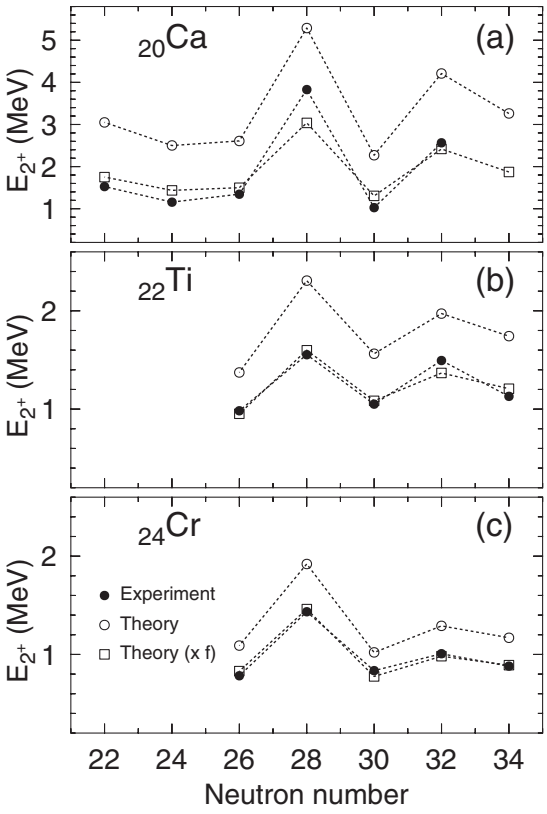

FIG. 4. Excitation energies of the 2_1^+ states for the Ca, Ti, and Cr isotopes; the experimental data are taken from [2] (Ca), [3–6] (Ti), and [7,8] (Cr). The values of the factor f are: 0.58 (Ca), 0.69 (Ti), and 0.76 (Cr).

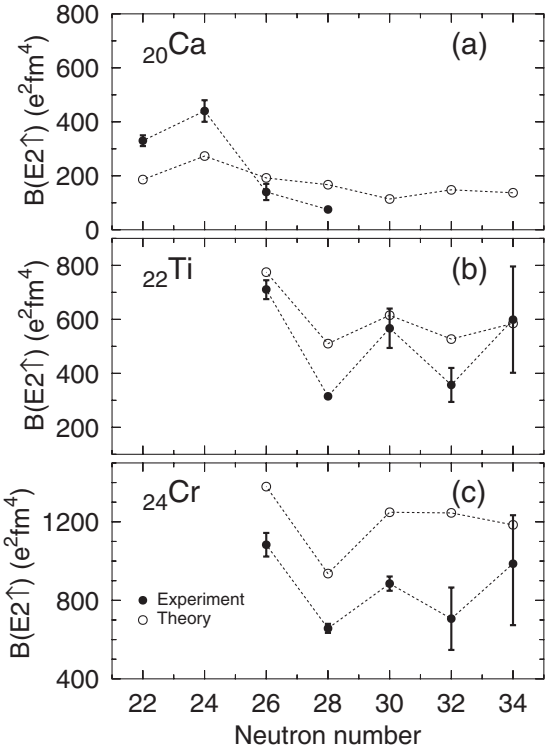

FIG. 5. $E2$ transition probabilities for the Ca, Ti, and Cr isotopes. The experimental data are taken from Ti [9] and Cr [10].

to bring the theoretical predictions in agreement with the experimental data. If we multiply our theoretical predictions by a factor 0.58 (Ca), 0.69 (Ti), and 0.76 (Cr), we obtain the results shown in the figure and now the agreement is spectacular. Concerning the question of the hypothetical shell closures at $N = 32$ and $N = 34$ from the pattern displayed by our results, we confirm the shell closure at $N = 32$. However, our results for ^{54}Ca do not support a shell closure for $N = 34$. To exclude additional triaxial effects, we have studied the $\beta - \gamma$ plane with a triaxial code in the VAP approach in the Calcium isotopes. The contour lines do not show any special features (softness) as a function of γ, and we do not expect drastic changes after an eventual triaxial angular momentum projection.

In Fig. 5, the $E2$ transition probabilities are displayed. As expected from Fig. 2, the largest values are found for the well deformed Cr isotopes and the smallest for the spherical Ca nuclei. Our results present a general trend similar to the experimental data and within a given isotopic chain; specially for the light isotones, the $B(E2)$'s are correlated with the relative energy of the $2+$ level: the higher the energy is, the smaller is the $B(E2)$. In general, our values are somewhat larger than the experimental ones. Probably, this is in part due to the Gogny force (and the Skyrme force too) that has the tendency to provide larger quadrupole moments than experimentally observed and partially to the already mentioned lack of triaxial shapes in our calculations. It is interesting to notice that our $B(E2)$ values qualitatively reproduce the experimental zigzag behavior in the Ti isotopes without any need to invoke effective charges. As mentioned in the introduction, shell model calculations with the usual values of the effective charges provide a flat behavior for the $B(E2)$ values of Ti. Though a readjustment of the effective charges leads to a certain improvement of the theoretical values [20], it remains to be investigated how these changes affect the $B(E2)$ values of other pf shell nuclei.

In conclusion, we present the first results of beyond-mean-field theories of the new generation where for the first time variation after projection effects were considered as well as simultaneous projection of angular momentum and particle number for the Gogny force. We have applied the theory to challenging problems and obtain a good agreement with the experimental excitation energies and a qualitative one with the transition probabilities. These results support a $N = 32$ shell closure and predict the nonexistence of a shell closure at $N = 34$. An added value of our results is the fact that the force parameters were fixed many years ago and that no effective charges are needed in our calculations.

The authors acknowledge discussions with L. M. Robledo and A. Jungclaus. This work has been supported in part by the DGI, Ministerio de Ciencia y Tecnologia, Spain, under Project No. FIS2004-06697.

[1] T. Otsuka *et al.*, Phys. Rev. Lett. **87**, 082502 (2001).
[2] A. Huck *et al.*, Phys. Rev. C **31**, 2226 (1985).
[3] S. N. Liddick *et al.*, Phys. Rev. Lett. **92**, 072502 (2004).
[4] R. V. F. Janssens *et al.*, Phys. Lett. B **546**, 55 (2002).
[5] S. N. Liddick *et al.*, Phys. Rev. C **70**, 064303 (2004).
[6] B. Fornal *et al.*, Phys. Rev. C **70**, 064304 (2004).
[7] J. I. Prisciandaro *et al.*, Nucl. Phys. A **682**, 200c (2001).
[8] J. I. Prisciandaro *et al.*, Phys. Lett. B **510**, 17 (2001).
[9] D.-C. Dinca *et al.*, Phys. Rev. C **71**, 041302(R) (2005).
[10] A. Bürger *et al.*, Phys. Lett. B **622**, 29 (2005).
[11] M. Honma *et al.*, Phys. Rev. C **65**, 061301(R) (2002).
[12] A. Poves *et al.*, Nucl. Phys. A **694**, 157 (2001).
[13] T. Otsuka *et al.*, Eur. Phys. J. A **15**, 151 (2002).
[14] M. Bender *et al.*, Rev. Mod. Phys. **75**, 121 (2003).
[15] R. Rodríguez-Guzmán *et al.*, Nucl. Phys. A **709**, 201 (2002).
[16] T. Niksic *et al.*, Phys. Rev. C **74**, 064309 (2006).
[17] M. Anguiano *et al.*, Phys. Lett. B **545**, 62 (2002).
[18] P. Ring and P. Schuck, *The Nuclear Many Body Problem* (Springer-Verlag, Berlin, 1980).
[19] K. W. Schmid, Prog. Part. Nucl. Phys. **52**, 565 (2004).
[20] A. Poves *et al.*, Phys. Rev. C **72**, 047302 (2005).
[21] J. Decharge and D. Gogny, Phys. Rev. C **21**, 1568 (1980).
[22] M. Anguiano *et al.*, Nucl. Phys. A **696**, 467 (2001).
[23] T. R. Rodriguez and J. L. Egido (to be published).
[24] J. L. Egido and L. M. Robledo, in *Lecture Notes in Physics*, edited by G. Lalazissis, P. Ring, and D. Vretenar (Springer-Verlag, Heidelberg, 2004), Vol. 641, p. 269.